Published in final edited form as:
J Mol Cell Cardiol. 2009 July ; 47(1): 121–132. doi:10.1016/j.yjmcc.2009.04.008.

Functional Role of CLC-2 Chloride Inward Rectifier Channels in Cardiac Sinoatrial Nodal Pacemaker Cells

Z. Maggie Huang[a,c], **Chaithra Prasad**[a,c], **Fiona C. Britton**[b,c], **Linda L. Ye**[a,c], **William J. Hatton**[a,c], and **Dayue Duan**[a,c,*]

[a] Department of Pharmacology, University of Nevada School of Medicine, Reno, Nevada 89557-0270, USA

[b] Department of Physiology and Cell Biology, University of Nevada School of Medicine, Reno, Nevada 89557-0270, USA

[c] Center of Biomedical Research Excellence, University of Nevada School of Medicine, Reno, Nevada 89557-0270, USA

Abstract

A novel Cl^- inward rectifier channel (Cl,ir) encoded by *ClC-2*, a member of the ClC voltage-gated Cl^- channel gene superfamily, has been recently discovered in cardiac myocytes of several species. However, the physiological role of Cl,ir channels in the heart remains unknown. In this study we tested the hypothesis that Cl,ir channels may play an important role in cardiac pacemaker activity. In isolated guinea-pig sinoatrial node (SAN) cells, Cl,ir current was activated by hyperpolarization and hypotonic cell swelling. RT-PCR and immunohistological analyses confirmed the molecular expression of *ClC-2* in guinea-pig SAN cells. Hypotonic stress increased the diastolic depolarization slope and decreased the maximum diastolic potential, action potential amplitude, APD_{50}, APD_{90}, and the cycle-length of the SAN cells. These effects were largely reversed by intracellular dialysis of anti-*ClC-2* antibody, which significantly inhibited Cl,ir current but not other pacemaker currents, including the hyperpolarization-activated non-selective cationic "funny" current (I_f), the L-type Ca^{2+} currents ($I_{Ca,L}$), the slowly-activating delayed rectifier I_{Ks} and the volume-regulated outwardly-rectifying Cl^- current ($I_{Cl,vol}$). Telemetry electrocardiograph studies in conscious ClC-2 knockout (*Clcn2*$^{-/-}$) mice revealed a decreased chronotropic response to acute exercise stress when compared to their age-matched *Clcn2*$^{+/+}$ and *Clcn2*$^{+/-}$ littermates. Targeted inactivation of ClC-2 does not alter intrinsic heart rate but prevented the positive chronotropic effect of acute exercise stress through a sympathetic regulation of ClC-2 channels. These results provide compelling evidence that *ClC-2*-encoded endogenous Cl,ir channels may play an important role in the regulation of cardiac pacemaker activity, which may become more prominent under stressed or pathological conditions.

Keywords

arrhythmia; cardiac electrophysiology; ion channels; sinoatrial node; transgenic mice

*Please send correspondence to: Dayue Duan, MD, PhD, FAHA, Laboratory of Functional Genomics and Proteomics, Center of Biomedical Research Excellence, Department of Pharmacology, University of Nevada School of Medicine, Manville Medical Building Room #9/MS 318, Reno, Nevada 89557-0270, Tel: (775) 784-4738, Fax: (775) 784-1620, e-mail: dduan@medicine.nevada.edu.

Introduction

The possible contribution of Cl^- currents to spontaneous cardiac action potentials was first described in multicellular preparations of Purkinje fibers by Carmeliet [1] and Hutter & Noble in 1961 [2]. Later, investigators from several laboratories observed the Cl^- dependence of the diastolic depolarization and action potential duration. They characterized a hyperpolarization-activated Cl^- current in multicellular preparations of rabbit sinoatrial node (SAN) [3–5]. However, the potential functional role of the hyperpolarization-activated Cl^- currents in cardiac pacemaker activity has been completely ignored due to serious doubts about the existence and functional role of any type of Cl^- channels in the heart [6,7].

Recently, a novel Cl^- inward rectifier channel (Cl,ir) was identified in cardiac atrial and ventricular myocytes of several species, including guinea-pig [8,9], mouse [9], and rat [8,10, 11]. The Cl,ir currents ($I_{Cl,ir}$) have characteristics of activation by hypotonic cell swelling and extracellular acidification, inward rectification, time-dependent slow activation, and Cd^{2+}-sensitive blockade [8–11]. These properties are very similar to the currents carried by the *ClC-2* channels expressed in heterologous system [12,13], suggesting Cl,ir may be encoded by the *ClC-2* gene, a member of the *ClC* voltage-gated chloride channel superfamily [12]. Additional studies confirmed the expression of *ClC-2* throughout the heart [14]. Upon expression in NIH/3T3 cells, cardiac *ClC-2* cloned from guinea-pig heart yielded currents similar to endogenous $I_{Cl,ir}$ in native cardiac myocytes of guinea-pig, supporting that *ClC-2* may be the gene responsible for the endogenous $I_{Cl,ir}$ in native cardiac cells [8].

The exact function of Cl,ir channels in the heart, however, remains to be elucidated. Because of its similarity to the pacemaker current I_f, in terms of time-dependent activation and inward rectification during membrane hyperpolarization, we hypothesize that Cl,ir channel may also exist in SAN cells and contribute to the pacemaker activity. To test this hypothesis, we first examined the functional and molecular expression of Cl,ir and *ClC-2* in the SAN cells and then further investigated the functional role of *ClC-2* in pacemaking activity using specific anti-*ClC-2* antibody. These results provide compelling evidence that the *ClC-2* encoded $I_{Cl,ir}$ in the SAN cells may contribute to the regulation of pacemaker activity of the heart, especially under stressed or pathological conditions.

Materials and Methods

This investigation conforms to the Guide for the Care and Use of Laboratory Animals (US National Institute of Health publication No. 85-23, revised 1996) and was in accordance with the institutional guidelines for animal care and use approved by the University of Nevada Institutional Animal Care and Use Committee.

SAN cell isolation

Single SAN cells were enzymatically isolated from guinea-pig heart as described [15]. Briefly, The guinea-pig SAN preparation was dissected along the anatomic land markers as delineated by surrounding crista terminalis, atrial septum, superior and inferior vena cava. The SAN region was translucent as compared to adjacent atria tissue.

Electrophysiological measurements

Whole-cell currents and action potentials were measured using the tight-seal whole-cell voltage-clamp and current-clamp techniques, respectively, as previously described [8,9]. Data acquisition and command potentials were controlled by pCLAMP 8.0 software (Axon Instruments). Whole-cell currents were filtered at 1 kHz and sampled at 5 kHz. Recording pipettes were prepared from borosilicate glass electrodes (1.5 mm o.d.) with tip resistance of

1–3 MΩ when filled with pipette solutions. After a tight seal between the cell membrane and the pipette tip (seal resistance >10 GΩ) had been formed, the membrane patch was ruptured with brief additional suction. The capacitive transients elicited by symmetrical 5-mV steps from 0 mV were recorded at 100 kHz for subsequent calculation of capacitance and access resistance. Input resistance was defined as the amplitude of the steady state voltage response divided by the current amplitude, and input conductance as the reciprocal value of input resistance. The cellular capacitance of the SAN cells ranged from 35~55 pF and averaged 46.3 ±2.2 pF (n=29). The mean input resistance was 0.57±0.06 GΩ, a value of the same order as that obtained by others [16–18]. To account for differences in cell size, whole-cell currents were normalized to cell capacitance, and the average data were reported as current densities (pA/pF). Series resistance (3–6 MΩ) was then compensated to minimize the duration of the capacitive surge on the current record during 5-mV hyperpolarizations from 0 mV, and over 70% compensation was usually obtained. To prevent contamination from the cationic inward rectifier I_{K1}, Ba^{2+} (2 mM) was continuously present in the extracellular bath solutions except for current clamp measurements. Hypotonic (230 mOsm/kg H_2O, measured by freezing-point depression) bath solution contained (mM): NaCl 100, KCl 5.4, $MgCl_2$ 1, $CaCl_2$ 1.8, $BaCl_2$ 2, NaH_2PO_4 0.33, N-(2-hydroxyethyl) piperazine-N′-(2-ethanesulphonic acid) (HEPES) 5, glucose 5.5, $[Cl^-]_o$=113; pH 7.4. In some experiments, 20 mM NaCl was replaced with equimolar concentration of CsCl. The isotonic and hypertonic bath solutions were the same as the hypotonic solution except the osmolarity was adjusted to 290 and 360 mOsm kg^{-1} H_2O, respectively, by adding mannitol. The pipette solution contained (mM): KCl 113, K-ATP 5, Na-GTP 0.1, ethylene-glycobis (b-aminoethyl ether)-N,N,N9,N9-tetraacetic acid (EGTA) 5, HEPES 5, $[Cl-]_i$ =113; pH 7.2, 290 mOsm kg^{-1} H_2O using mannitol adjustment. In experiments described in Figure 1C, cations in the intracellular and extracellular solutions were replaced by the large impermeant cation, N-methyl-D-glucamine (NMDG) and pipette solution $[Cl^-]$ was changed to 25 mM by replacing 88 mM NMDG-Cl with equimolar NMDG-aspartate. For action potential recordings as described in Figure 4, low $[Cl^-]_i$ (25 mM) was used and NMDG was replaced by equimolar of K^+. For intracellular dialysis experiments, anti-*ClC-2* antibody (Ab) (Alomone Labs) was included in the pipette solution (final concentration, 3 μg/ml). The voltage clamp and current clamp protocols used in different experiments are described in the figure legends. Action potential amplitude (APA) is measured as the peak positive potential minus the maximum diastolic potential (MDP). The diastolic depolarization slope (DDs, in mV/s) was measured over the 100 ms time interval starting at MDP. Action potential durations at 50% and 90% repolarization to the MDP were measured as APD_{50} and APD_{90}, which represents the time interval between the time of APA and the time to a 50% or 90% decrease of the APA to the MDP, respectively [2]. Experiments were conducted under room temperature (22–24°C).

Immunohistochemistry

The cellular localization of *ClC-2* protein in both cryostat sections of SAN tissue and acutely dispersed cardiac SAN cells was determined using immunofluorescent and confocal microscopy.

Immunohistochemistry in cryostat sections of guinea-pig SAN—The guinea-pig SAN region was dissected as described above. The tissue was fixed in 4% paraformaldehyde for 1 hr, washed with PBS 3×10 min, and cryoprotected in 20% sucrose in PBS overnight at 4 °C. The tissue was then embedded in Tissue Tek (Miles, IL, USA) embedding medium and 20% sucrose in PBS (1:1 vol/vol) and rapidly frozen in isopentane precooled in liquid nitrogen. Cryosections were cut with a Leica CM 3500 cryostat at a thickness of 10 μm and collected on Surgipath microscope slides (Richmond, IL, USA). Sections were washed 3×10 min with PBS to remove mounting medium then immunohistochemically stained with a polyclonal *ClC-2* antibody (Ab) raised in rabbit (1:200, Alomone Labs, Jerusalem, Israel) [19] and a

monoclonal anti-Connexin43 (1:500, Milipore, CA) [20,21]. DAPI (Vector Laboratories Inc., Burlingame, CA) was used for mount and nuclei labeling. The permeabilization step was achieved by 1-hr incubation with 0.3% Triton-X100 (Sigma). Immunohistochemically labeled sections were examined using a TE 300 inverted fluorescent microscope (Nikon, USA) equipped with both differential interference (DIC) optics and filter cubes with excitation/emission wavelengths appropriate for Alexa 488 and 546. Confocal micrographs were acquired using a Bio-Rad Radiance 2100 Laser scanning confocal microscope with LaserSharp 2000 software (Bio-Rad, Hercules, CA, USA). Confocal composites were constructed from scans of 14 optical sections through a depth of 10 μm (14 × 0.71μm). Final images were constructed using Adobe Photoshop CS software.

Immunocytochemistry in acutely dispersed SAN cells—Cells were allowed to settle for 20 minutes on glass bottomed tissue culture plates precoated with Cell Tak (BD Biosciences, MA) as per manufacturer's instructions. Excess dispersion media was removed and cells were fixed with 4% paraformoldehyde and permeabilized with 0.1% Triton-X100. The cells were incubated with 1.5% neonatal goat serum for 1 hr then incubated overnight at 4 °C with anti-*ClC-2* Ab (1:200). Following incubation cells were washed with PBS (2×10 min) then incubated for 1 hr with Alexa 488 (green fluorescence) conjugated anti rabbit IgG secondary antibody (Molecular Probes, Eugene, OR). Cells incubated with (a) TBS instead of anti-*ClC-2* Ab or (b) pre-absorbed Ab with appropriate antigen (1 hr) were used as negative controls. The labeled cells were examined on a TE 300 inverted fluorescent microscope (Nikon, USA) equipped with both differential interference (DIC) optics and filter cubes with excitation/emission wavelengths appropriate for Alexa 488. DIC and fluorescent digital photomicrographs were acquired using a Spot RT Slider CCD camera (Diagnostic Instruments, MI, USA) using proprietary software. Final images were constructed using Adobe Photoshop CS software.

Reverse transcription-polymerase chain reaction (RT-PCR)

RT-PCR of RNA from enzymatically dispersed individual SAN cells was performed as previously described [9,14]. The forward primer 5′-TGGGAGGAGCAGCAGCTGAA-3′ and reverse primer 5′-CAGAGTGCATGCACCTCTGTGGT-3′) are specific for gp*ClC-2* (nucleotides 2481 to 2788, GenBank accession No. AF113529), generating a 308-nucleotide amplification product.

ClC-2 knockout (*Clcn2*$^{-/-}$) mice

Homozygous *Clcn2*$^{-/-}$ mice were generated in the Transgenic Center at the University of Nevada, Reno by mating heterozygous (*Clcn2*$^{+/-}$) breeders (generously provided by Dr. James Melvin at University of Rochester [22]) to *Clcn2*$^{+/-}$ siblings. Genotypes of the mice were confirmed by polymerase chain reaction (PCR) on tail DNA as described [22].

Radiotelemetry electrocardiography (ECG) recording in conscious mice

ECG, heart rate (HR), body temperature and activity were measured, collected and stored to hard disk of an IBM-compatible computer using the Data Sciences International radiotelemetry data acquisition system (Dataquest A.R.T. version 2.2, Data Sciences International, St Paul, MN). Briefly, 8-week-old mice were anesthetized with sodium pentobarbital (50~100 mg/kg, ip) and an incision (1.5 cm) was made along the midline immediately caudal to the xyphoid space for the subcutaneous placement of the body of the implantable transmitter (ETA-F20). The two insulated stainless-steel biopotential leads (0.5 mm diameter) of the transmitter were cut to the appropriate length and placed subcutaneously into the small incisions (0.5 cm) in the lead II configuration (negative lead to the right shoulder and the positive lead to the left of the xyphoid space and caudal to the rib cage). The device was included in the closing suture (4-0

non-absorbable) to prevent displacement. Experiments were initiated 48 hrs after recovery from the surgical procedure. Mice were housed in individual cages with unrestricted access to standard chow and drinking water and were exposed to a light-dark circle of 12-hours (light time: 8 AM – 8PM) in a thermostatically controlled room (24±1°C). ECG were monitored both under resting conditions in the cage and during treadmill exercises.

Treadmill Exercise Regimen

The rodent Treadmill Simplex II (Columbus Instruments, Columbus, Ohio) that has an adjustable speed (0–100m/min), shock bars with adjustable amperage (0–2mA) at the back of the belt, and an on-and-off shock bar switch was used for exercise regimens. The treadmill exercise protocol was composed of 1) Rest: acclimation period at 0–2 m/min, incline 0 ° for 5 min; 2) Walk: walking period at 5m/min, incline 0 ° for 5 min; 3) Run: running period at 10 m/min, uphill incline 4° for 5 min followed by a faster running period at 15 m/min, uphill incline 8 ° for 5 min. The mice were continuously monitored and the exercise was terminated once the animal showed signs of exhaustion when mice stopped at the shock bar or failed to get back to the treadmill for >10 sec. The mice in all groups were acclimated (0–2 m/min, incline 0 ° for 5 min) on the treadmill twice a week for 2 weeks before the implantation of the telemetry probe. The exercise regimen resumed 2 days after surgery. The mice were monitored with the telemetry ECG system for 10 minutes every two hours at rest and continually during the treadmill exercise test. ECG parameters were measured using an end-fit method incorporated with the ECG analysis software (V3.2.2, Data Sciences International). The QT interval was corrected (QTc) for a heart rate (HR) of 600 bpm (R-R = 100 ms), a value near the physiologic HR in mice, using the following formula: $QTc = QT/(RR/100)^{1/2}$ as previously described [23].

Statistical Analysis

Data were expressed as mean ± S.E. Statistical comparisons were performed either by Student's *t* test when only two groups were compared or by analysis of variance (ANOVA) with Scheffé contrasts for group data. A two-tailed probability (P) of ≤ 0.05 is considered statistically significant.

Results

Functional expression of $I_{Cl,ir}$ in guinea-pig single SAN cells

Although it has been previously shown that $I_{Cl,ir}$ is present in a small portion (~10%) of guinea-pig atrial and ventricular myocytes [8,9], it is not known whether Cl,ir is functionally expressed in the SAN pacemaker cells. Therefore, we first examined whether $I_{Cl,ir}$ is also present in guinea-pig SAN cells. Figure 1A shows typical SAN cells (indicated by arrows) isolated from the SAN region of guinea-pig heart. The SAN cells were small, spindle shaped, without or with very mild striations, in contrast to adjacent well-striated bigger atrial cells. Figure 1B shows representative whole-cell current traces recorded from the SAN cells under isotonic and hypotonic conditions with cations (Na^+ and K^+) in the extracellular solutions. Cells were held at −60mV and test potentials were applied at an interval of 10 sec from −160 mV to +20 mV for 2 sec in +20 mV increments. Under isotonic conditions (panel **a**) a slowly activating inward current was elicited upon hyperpolarization. Exposure of the same cell to hypotonic extracellular solution caused cell swelling [9,24,25] and an increase in the inward current amplitude (panel **b**). The difference current caused by hypotonic challenge is shown in panel **e**. Subsequent exposure of the cell to 20 mM CsCl to block I_f [26] caused a significant decrease in the inward current amplitude (panel **c**). The difference current shown in panel **f** is the typical Cs^+-sensitive I_f [26], which was used also as one of the criteria of the SAN cells. The Cs^+-insensitive current was significantly reduced by 0.2 mM extracellular Cd^{2+} (Figure 1B,d&g). The Cd^{2+}-sensitive, time-dependent and slowly-activating inward current had an inwardly-

rectifying *I–V* relationship and reversed at −3 mV, which was very close to the predicted equilibrium potential of Cl^- (E_{Cl}=0 mV) with a symmetrical Cl^- gradient ($[Cl^-]_o$/$[Cl^-]_i$=113/113 mM). These characteristics are very similar to those of $I_{Cl,ir}$ in guinea-pig atrial and ventricular myocytes [8,9]. It can also be seen from Figure 1B,g that the other component of the Cd^{2+}-sensitive transient inward current was activated at more positive membrane potentials (>−40 mV) with characteristics of $I_{Ca,L}$ [27], which were more apparent in traces at higher gain (not shown).

To further determine the ion selectivity of the slowly-activating and inwardly-rectifying Cs^+-insensitive current, all cations in the extracellular and intracellular solutions were replaced with the large impermeant cation NMDG, and pipette solution [Cl^-] was changed to 25 mM, which is within the range of physiological intracellular Cl^- concentrations (20–30 mM) [28]. With Cl^- as the only permeant ion, hyperpolarization still activated a slowly activating inward current, which was blocked by Cd^{2+} (Figure 1C). The mean *I–V* curve of the swelling-induced Cd^{2+}-sensitive current is shown in Figure 1C,d. This inward current was cation-independent and reversed at membrane potentials (−37.4±2.6 mV, n=5) close to E_{Cl} (−38.8 mV) as estimated by Nernst Equation calculation, suggesting the inward current is carried by Cl^-. Therefore, the Cd^{2+}-sensitive inward Cl^- current in the SAN cells shares many properties with $I_{Cl,ir}$ recorded in guinea-pig atrial and ventricular myocytes, including the time-dependent activation, inward rectification, Cd^{2+}-sensitivity, cation-independence and a reversal potential close to E_{Cl}, strongly indicating that this current may be the same $I_{Cl,ir}$ as seen in guinea-pig atrial and ventricular myocytes [8,9]. Similar results were obtained in all 5 (5 of 5, 100%) SAN cells studied under the same conditions.

Molecular expression of *ClC-2* in guinea-pig SAN cells—Our previous studies have identified *ClC-2* as the gene encoding the endogenous Cl,ir in guinea-pig atrial and ventricular myocytes [8,9,14]. In this study, immunohistochemistry and RT-PCR were used to further examine whether *ClC-2* is expressed in SAN cells.

It has been reported that connexin 43 (Cx43) is expressed in the atria and ventricle but not in the central SAN region [20,21], and the SAN region had a higher nuclei density when compared to the atria [29]. Therefore, in this study both anti-Cx43 Ab and the nuclei marker DAPI were used to delineate the SAN region from the atrial (AT) septum (dashed white line). Consistent with previous observations, as shown in Figure 2A, while the adjacent atrial septum was positively labelled with anti-Cx43 (red in Figure 2A,a) the SAN was negative with anti-Cx43 labelling and had higher DAPI staining density than the adjacent atrial septum (blue in Figure 2A,b). Both atrial and SAN regions were labelled with anti-*ClC-2* Ab (green Figure 2A,c). The merged image of *ClC-2* (green), Cx43 (red), and DAPI (blue) in Figure 2A,d clearly shows the expression of *ClC-2* in the Cx43 negative and densely nucleated SAN region.

To further directly confirm the expression of *ClC-2* in single SAN cells, RT-PCR and immunocytochemistry were applied to the acutely dispersed guinea-pig SAN cells. As shown in Figure 2B, RT-PCR using mRNA extracted from isolated single SAN cells amplified a 307 base pair (bp) product specific for *ClC-2*. This product was sequenced to confirm its identity. Furthermore, immunolabelling of *ClC-2* in the acutely dispersed single SAN cells also demonstrated that *ClC-2* is expressed in SAN cells (green fluorescence in Figure 2C,b).

Effects of anti-*ClC-2* antibody on $I_{Cl,ir}$ and action potential in guinea-pig SAN cells—Antibodies specifically against ion channels have been widely used as specific ion channel blockers [8,30,31]. In our previous study, anti-*ClC-2* Ab inhibited native $I_{Cl,ir}$ in rat and guinea-pig ventricular myocytes, as well as *ClC-2* currents expressed in NIH/3T3 cells [8]. Therefore, we used the same specific approach to test whether anti-*ClC-2* Ab would

functionally block the whole-cell $I_{Cl,ir}$ and affect the spontaneous action potential in the SAN cells.

Whole-cell patch-clamp technique was applied to record whole-cell current (voltage-clamp mode) and spontaneous action potential (current-clamp mode) from SAN cells. In the test group anti-*ClC-2* Ab (3 μg/ml) was dialyzed into the SAN cells through the pipette solution while in the control group pipette solutions contained the same amount of pre-absorbed anti-*ClC-2* sera or no antibody.

In the first test group, whole-cell currents were recorded from SAN cells in the presence of anti-*ClC-2* Ab when the cells were first exposed to isotonic solutions for 10 min (Figure 3**Aa**,) and then to hypotonic solutions for 20 min (Figure 3**A,b**). Under these conditions two types of inward currents were observed. One is the slowly activated typical I_f as seen in Figure 1**B,f**. The other is the typical $I_{Ca,L}$, which is a transient inward current activated at more positive potentials. The difference current caused by hypotonic cell swelling is shown in Figure 3A,c. The mean *I–V* curves (n=5) under isotonic and hypotonic conditions (Figure 3 A,**d**) were almost identical, indicating that cell swelling failed to activate any current in the presence of intracellular anti-*ClC-2* Ab. This is in clear contrast to the results as shown in Figure 1B where cell swelling activated $I_{Cl,ir}$ in the absence of anti-*ClC-2* Ab. These results indicated that a) I_f and $I_{Ca,L}$ were not activated by hypotonic cell swelling; b) anti-*ClC-2* Ab had no effects on the basal currents including I_f and $I_{Ca,L}$; c) $I_{Cl,ir}$ may be minimally activated under isotonic conditions; and d) anti-*ClC-2* Ab prevented the hypotonic activation of $I_{Cl,ir}$ in SAN cells.

In the second test group, the SAN cells were first exposed to hypotonic solution before the whole-cell configuration for about 20 min to fully activate $I_{Cl,ir}$ [8,9]. The whole-cell currents were recorded immediately after the break of the cell membrane (Figure 3**B,a**). Dialysis of the cell with anti-*ClC-2* Ab for 20 min resulted in a decrease in inward current amplitude (Figure 3**B,b**). The difference current caused by dialysis of anti-*ClC-2* Ab is shown in Figure 3**B,c**. The mean *I–V* curve of the currents inhibited by anti-*ClC-2* Ab in Figure 3**B,d** was similar to the *I–V* curve of $I_{Cl,ir}$ in Figure 1**C,d**. Again, the typical $I_{Ca,L}$ and I_f(**b**) were not affected by anti-*ClC-2* Ab. These results indicated that anti-*ClC-2* Ab selectively inhibited the hypotonic activation of $I_{Cl,ir}$ but not the I_f and $I_{Ca,L}$ in SAN cells. These results further support the notion that *ClC-2* channels are responsible for $I_{Cl,ir}$ in the guinea-pig SAN cells.

To examine the consequences of $I_{Cl,ir}$ inhibition by anti-*ClC-2* Ab on the action potential profile and pacemaker activity we recorded spontaneous action potentials from guinea-pig SAN cells using current-clamp mode under isotonic and hypotonic conditions. As shown in Figure 4 and Table 1, in the control groups with pipette solutions containing either no anti-*ClC-2* Ab (Figure 4A) or pre-absorbed anti-*ClC-2* sera (Figure 4B) exposure of the SAN cells to hypotonic solutions for 20 min caused an increase in the DDs and a decrease in the MDP, action potential amplitude (APA), APD_{50}, APD_{90}, and the cycle-length (CL). In the test group with pipette solutions containing anti-*ClC-2* Ab (Figure 4C), the SAN cells were exposed to either isotonic (Figure 4C) or hypotonic solutions (Figure 4D) for 20 min before whole-cell configuration was formed. Under isotonic conditions, as shown in Figure 4C, the spontaneous action potentials recorded at the beginning right after the formation of the whole-cell configuration were comparable to those recorded under the same isotonic conditions in the control groups (Figure 4A,a and B,a). Dialysis of the cells with anti-*ClC-2* Ab for 20 min under isotonic conditions caused no significant changes in the action potentials (Figure 4C, b&d). Similar results were observed in a total of 4 different SAN cells (Table 1). The lack of anti-*ClC-2* Ab effect on SAN action potentials may be explained by the fact that 1) it has been well-established in cardiac and non-cardiac cells that ClC-2 channels are normally inactive under isotonic conditions [8, 9,12,13], and 2) $I_{Cl,ir}$ is hardly activated at membrane potentials more positive than −60 mV under isotonic conditions in SAN cells (see Figures 1 and 3). Under hypotonic conditions, as

shown in Figure 4D and Table 1, the spontaneous action potentials recorded at the beginning right after the formation of the whole-cell configuration were comparable to those recorded under hypotonic conditions in the control groups (Figure 4A,b and B,b). Dialysis of the cells with anti-*ClC-2* Ab for 20 min, which corresponds to the time when $I_{Cl,ir}$ was significantly inhibited (Figure 3B,b), reversed the hypotonic stress-induced changes in DDs, MDP, APA, APD_{90} and CL of the action potential (Figure 4D,b and Table 1). But the shortening of APD_{50} was not significantly changed (Table 1), suggesting anti-*ClC-2* Ab may have no significant effect on the major repolarizing currents. This was further confirmed by the fact that dialysis of anti-*ClC-2* Ab had no effect on the slowly-activating delayed rectifier I_{Ks} and the volume-regulated outwardly-rectifying Cl^- current ($I_{Cl,vol}$), two major repolarizing currents which can also be activated by hypotonic cell swelling [9,32,33] in guinea-pig SAN and ventricular cells (data not shown). These results strongly suggest that the activation of *ClC-2* channels may contribute mainly to the changes in the diastolic depolarization and firing rate of SAN pacemaker activity but very little to the repolarization at positive potentials during hypotonic stress.

Effects of targeted inactivation of ClC-2 on ECG under rest and stressed conditions

To further test our hypothesis that ClC-2 channels may play an important role in the regulation of pacemaker activity and cardiac function, $Clcn2^{-/-}$ mice [22] were used to address the question whether targeted inactivation of *ClC-2* gene causes significant changes in cardiac electrophysiology *in vivo* under rest and stressed conditions.

To eliminate the influence of changes in the heart rate and cardiac performance under anesthetized status, a radiotelemetry system was used to continuously monitor the ECG, body temperature and activity of $Clcn2^{-/-}$ mice and their age- and gender-matched wild-type ($Clcn2^{+/+}$) and heterozygous ($Clcn2^{+/-}$) littermates under conscious conditions. At the age of 8 weeks, telemetry transmitters were implanted (see Materials and Methods for surgical procedures). The body weight of the $Clcn2^{-/-}$ mice (29.67±0.61g, n=7) was not significantly different from $Clcn2^{+/-}$ (28.18±1.30g, n=5) and $Clcn2^{+/+}$ (31.87±1.24g, n=6) mice. The resting heart rate (HR) of the $Clcn2^{-/-}$ mice (653±13 bpm, n=7) was slower but not significantly different from $Clcn2^{+/-}$ (710±34 bpm, n=5, $P>0.1$) and $Clcn2^{+/+}$ (718±30 bpm, n=6, $P>0.05$) mice. No significant differences in the resting ECG parameters, including PQ, QRS, ST, QT, and the QT interval corrected for the heart rate increase (QTc), were found in these littermates (data not shown). This may be explained by the fact that $I_{Cl,ir}$ through ClC-2 channels under basal or isotonic conditions is relatively small. It has been known that, however, $I_{Cl,ir}$ is activated in a larger scale by cell swelling [8,9], acidosis [10,11,34], and PKA phosphorylation [35].

To detect cardiac abnormalities that are not readily apparent at rest cardiovascular stress in response to treadmill exercise is frequently used [36]. However, a change in intrinsic HR during chronic intensive treadmill exercise may be due to changes in ion channel expression or activity related to training on the treadmill over time but not a result of targeted gene knockout *per se* [37]. In our study, we were interested in a controlled exercise regimen that could induce acute cardiac stress in a manner that would allow for a quantitative assessment of performance and reproducibility of the observed changes in HR over a reasonable period of time in the same mouse throughout the exercise protocol. Therefore, we adapted a treadmill exercise protocol for mice from Fewell et al [36]. The mice with telemetry implants were subjected to exercise on treadmill (maximum intensity: 15 m/min, uphill incline 8° for 5 min). ECG was monitored during the treadmill exercise using the telemetry ECG system. Figure 5A shows the typical recordings from the three groups during the treadmill exercise. Changes in the mean heart rate measured during the treadmill exercise period are summarized in Fig. 5B. Walking at 5 m/min, incline 0 ° for 5 min and running at 15 m/min, uphill incline 8° for 5 min caused a significant

increase in HR in *Clcn2*$^{+/+}$ (n=6) and *Clcn2*$^{+/-}$ (n=5) mice. Under the same conditions, however, the increase in HR of the *Clcn2*$^{-/-}$ mice (n=7) was significantly less than that in the *Clcn2*$^{+/+}$ and *Clcn2*$^{+/-}$ littermates (Figure 5). Knockout of ClC-2 gene mainly caused a slower heart rate without altering QTc or any other ECG parameters (data not shown).

To further determine whether the differences in exercise-induced changes in HR between the *Clcn2*$^{+/+}$ and *Clcn2*$^{-/-}$ mice were due to altered intrinsic heart rate (IHR) by ClC-2 knockout or specific effect of autonomic regulation on the SA node region of these mouse hearts, vagal and sympathetic function and IHR were measured by determining the response to atropine (0.5 mg/Kg) and propranolol (1 mg/Kg). ECG was recorded before and 10 min after intraperitoneal injection of the drugs. The mice were then immediately subjected to the same exercise protocol as described above. The IHR was evaluated after the combined treatment with propranolol and atropine. As shown in Figure 5C, blockade of vagal input by atropine increased basal HR of both *Clcn2*$^{+/+}$ and *Clcn2*$^{-/-}$ mice. In the presence of atropine acute exercise (walking and running) further significantly increased HR of the *ClCn2*$^{+/+}$ mice but not the *Clcn2*$^{-/-}$ mice. During exercise HR of the *ClCn2*$^{-/-}$ mice was significantly slower than that of the *ClCn2*$^{+/+}$ mice. When adrenergic input was blocked by propranolol, however, no significant difference in the resting HR was observed in these two groups of mice and exercise failed to increase HR in these mice. When both vagal and adrenergic inputs were blocked by combined administration of atropine and propranolol no significant differences were observed in the IHR between *ClCn2*$^{+/+}$ mice and *ClCn2*$^{-/-}$ mice. Exercise failed to cause any changes in HR in these mice. Therefore, regardless of the treatment, exercise caused no significant changes in HR of the *Clcn2*$^{-/-}$ mice. These results indicate that 1) ClC-2 knockout does not alter IHR and 2) sympathetic regulation of ClC-2 channels may play an important role in the positive chronotropic response to acute exercise stress.

Discussion

The results from this study provide novel experimental evidence for the molecular and functional expression of the *ClC-2* encoded Cl,ir channels in SAN cells and their functional role in the regulation of SAN cell pacemaker activity and heart rate under stressed conditions.

Cl,ir and *ClC-2* in SAN Cells

Early studies using ion-substitution strategies in multicellualr Purkinje fibers and SAN tissues provided initial experimental evidence for the potential physiological role of Cl^- and other anions in the regulation of membrane potentials, the diastolic depolarization and action potential duration of cardiac cells [1–3,5]. In 1961 Hutter & Noble [2] reported that upon the substitution of extracellular Cl^- by impermeant anions the heart rate transiently increased and then eventually decreased to between 40 and 90 % of that found in Cl^- solution. The replacement of Cl^- by permeant anions caused either an arrest or an initial slowing followed by acceleration of the rhythm. These changes were explained by the passive movement of anions during the action potential, assuming that the E_{Cl} was −50 mV [2]. Later, de Mello [5] and Noma & Irisawa [3] independently reported the Cl^--dependence of the diastolic depolarization in multicellular preparations of rabbit SAN tissue. Seyama [38] also reported that 9 % of the total membrane conductance of the resting potential is carried by Cl^-. In 1979, using the voltage-clamp technique Seyama [4] identified a time- and voltage-dependent inwardly rectifying Cl^- current in SAN cells of rabbit heart. This inwardly rectifying Cl^- current was only activated by membrane potentials more negative than −60 mV and might contribute to the diastolic depolarization. Eliminating this current component by a replacement of Cl^- with less permeable acetate caused a reduction in frequency of SAN rhythm and an increase in the amplitude of the action potential [4]. Later a similar Cl^- current was reported in frog sinus venosus [39]. Unfortunately, the biophysical and molecular properties of the

hyperpolarization-activated inwardly rectifying Cl^- channels have never been further characterized. Instead, a later study found that substitution of extracellular Cl^- with larger anions including isethionate, glutamate, acetate, and aspartate, reduced the amplitude of I_f without changing the reversal potential and substitution with small anions such as iodide or nitrate supported an intact I_f [40]. Therefore, the possible important role of the hyperpolarization-activated Cl^- current described in the 1960s and 1970s has been either disputed [40] or ignored [6,7]. Very little is known about Cl,ir channels and their potential functional role in the heart although recent efforts in the last twenty years have characterized the properties of several Cl^-channels in the heart at the cellular and molecular levels [6].

In this study, we observed an $I_{Cl,ir}$, in guinea-pig SAN cells. $I_{Cl,ir}$ is activated slowly upon cell membrane hyperpolarization and hypotonic challenge, has a strong inward rectification under symmetrical Cl^- conditions with a reversal potential close to the predicted value of E_{Cl}, and is inhibited by Cd^{2+}. All these properties are identical to those of $I_{Cl,ir}$ in atrial and ventricular myocytes of several species, including guinea-pig [8], rat [8–11], and mouse [9]. $I_{Cl,ir}$ is neither a part of the I_f nor a result of Cl^- regulation of the I_f activity [40] in SAN cells because a) $I_{Cl,ir}$ can be recorded in the presence of a strong I_f blocker (20 mM Cs^+) and in the absence of permeable cations; b) the reversal potential of $I_{Cl,ir}$is close to the predicted E_{Cl}, suggesting the inward current is carried by Cl^-, not by cations; c) $I_{Cl,ir}$ but not I_f can be inhibited by Cd^{2+}; and d) $I_{Cl,ir}$ but not I_f is specifically inhibited by anti-*ClC-2* Ab.

Our data from RT-PCR and immunohistochemistry provided direct evidence for the expression of *ClC-2* in SAN cells. In addition, dialysis of anti-*ClC-2* Ab but not the inactivated pre-absorbed Ab caused an inhibition of $I_{Cl,ir}$ but not I_f, $I_{Ca,L}$, I_{Ks} and $I_{Cl.vol}$. These results further support that *ClC-2* is the gene responsible for the endogenous Cl,ir channels not only in atrial and ventricular myocytes [8,14] but also in the SAN cells and that the Cl,ir in SAN cells may contribute to the regulation of pacemaker activity of the heart. Interestingly, the prevalence of functional endogenous $I_{Cl,ir}$ in the SAN cells (28/35, 80%) is apparently higher than that in the atrial or ventricular myocytes. Whether this difference is due to the higher molecular expression or the different activation mechanisms is a legitimate question which may be very difficult to get a clear answer. The first glance at the immunohistochemistry data shown in Figure 2 reveals no significant difference between the SAN and atrial tissues. Theoretically, a Western blot of membrane fractions would help to quantitatively analyze the differences in the protein expression of ClC-2 in the SAN cells and the atrial myocytes. But, practically, in order to carry out the Western blot analysis on the isolated membrane fractions from SAN cells it would need to collect enough SAN cells from the guinea-pig heart, which means not only a requirement for a pool of tens of hearts but also an isolation and selection of true SAN cells without contamination from the adjacent atrial cells. This is an extremely difficult task to accomplish. Although the confocal images of the SAN cells and atrail or ventricular myocytes would provide information on the subcellular distribution of ClC-2 channels in these cells it would not be able to give quantitative information for a decisive conclusion on the dynamic distribution of the ClC-2 channel protein and the relationship between the distribution and the function of the channels.

Physiological role of Cl,ir channels in the heart

Because the E_{Cl} in cardiac cells under physiological conditions ranges between −65 to −35 mV [28,41] which is very close to the MDP of SAN cells, the contribution of $I_{Cl,ir}$ to SAN cell action potential is unique and also more complicated than the activation of I_f and other cation currents. When the membrane potential is negative to E_{Cl}, opening of Cl,ir channel may conduct an inward current (Cl^- efflux), which will depolarize the MDP and increase the DDs. At the beginning of diastolic depolarization, the impedance of the cell is very large and activation of a small current may contribute significantly to the depolarization of the action

potential [42]. Therefore, both the smaller instantaneous $I_{Cl,ir}$ activated at membrane potentials near the MDP and the larger time-dependent $I_{Cl,ir}$ activated at membrane potentials more negative than the MDP may contribute pacemaker current to the phase 4 depolarization of the action potential of SAN cells. When the membrane potential is positive to E_{Cl}, opening of Cl,ir channel may conduct an outward current (Cl^- influx) and make the membrane potential (possibly including the MDP) more negative. But the inward rectification property of Cl,ir may limit the amplitude of the outward current and its contribution to repolarization and APD. Since the MDP may be determined normally by multiple mechanisms [43–45] such as I_f, I_{sus}, $I_{Ca.T}$, $I_{Ca,L}$, I_{NCX}, and possibly $I_{Cl.Ca}$ [46] and $I_{Cl.swell}$ [47], the contribution of changes in $I_{Cl,ir}$ to the MDP during hypotonic stress may be further complicated by changes in other ionic currents which may also responded to hypotonic cell swelling such as $I_{Cl.swell}$ [6,47] and I_{Ks} [33]. In addition, activation of $I_{Cl,ir}$ may also cause a dynamic change in the E_{Cl} [48]. The analysis of the relationship of the activation of $I_{Cl,ir}$ to the E_{Cl} and the consequent role of this relationship in determining the MDP has been limited by the lack of potent and specific $I_{Cl,ir}$ blocker. The identification of *ClC-2* as the gene responsible for Cl,ir channels in the heart and the availability of specific anti-*ClC-2* Ab provided us specific approach to effectively examine the functional role of Cl,ir in the heart.

In the isolated SAN cells, dialysis of anti-*ClC-2* Ab through the pipette solution for 20 min inhibited $I_{Cl,ir}$ (Figure 3B) and reversed the hypotonic stress-induced increase in DDs and decrease in MDP, APA, APD_{90}, and CL under hypotonic conditions, suggesting that $I_{Cl,ir}$ may play a role in the regulation of diastolic depolarization and the firing rate of spontaneous action potential of SAN cells under stressed conditions. Anti-*ClC-2* Ab, however, did not have significant effect on the hypotonicity-induced shortening of APD_{50} (see Table 1). This may suggest that the contribution of the $I_{Cl,ir}$ to the repolarization at positive potentials is rather small because of its inward rectification property. These data may provide new mechanistic insight into the tonicity regulation of spontaneous beating rate in guinea–pig SAN reported by Ohba in 1986 [49]. In that study it was found that decreasing the osmolarity by 30% increased the heart rate by 6% and increasing the osmolarity to 130, 150, and 170% decreased the heart rate to 94, 89, and 73%, respectively [49].

As mentioned above it is possible that the observed anti-*ClC-2* Ab-induced reduction in pacemaker activity under hypotonic conditions may be due to a non-specific block of hypotonic activation of I_{Ks} [33] and $I_{Cl,vol}$ [47]. But we found that anti-*ClC-2* Ab failed to affect I_{Ks} and $I_{Cl,vol}$ under either isotonic or hypotonic conditions (data not shown). These results are consistent with the observation that anti-*ClC-2* Ab has no effect on APD_{50} and strongly suggest that the activation of ClC-2 channels may play an important role in the diastolic depolarization and firing rate of SAN pacemaker activity but have very little impact on the repolarization at positive potentials during hypotonic stress. In addition, dialysis of pre-absorbed anti-ClC-2 Ab did not cause any changes in the response of the SAN pacemaker activity to hypotonic stress (Figure 4A and B) or in the hypotonic activation of $I_{Cl,ir}$ (please see Fig. 9 of reference 8). Therefore, it is highly unlikely that the anti-*ClC-2* Ab-induced reduction in the current amplitude of $I_{Cl,ir}$ (Figure 3B) and pacemaker activity (Figure 4 and Table 1) in the SAN cells under hypotonic conditions are not due to the effects of anti-*ClC-2* Ab but the potential effects of dialysis with pipette solutions *per se*.

In agreement with our findings in the isolated cells, targeted inactivation of ClC-2 channels caused a decrease in HR, especially under exercise stress. The resting HR of the $Clcn2^{-/-}$ mice was slower but not significantly different from the $Clcn2^{+/+}$ and $Clcn2^{+/-}$ mice. This may be explained by the fact that $I_{Cl,ir}$ through ClC-2 channels under basal or isotonic conditions is relatively small. It has been known that, however, $I_{Cl,ir}$ is activated in a larger scale by cell swelling [8,9], acidosis [10,11,34], and PKA phosphorylation [35]. Indeed, hypoxia, ischemia, and acidosis have consistently been shown to increase automaticity and cause lethal

arrhythmias, although the mechanism has remained obscure [6,50]. Activation of $I_{Cl,ir}$ may explain, at least in part, the increase in automaticity under these stressed or pathological conditions [10,11]. In the present study, we found that during acute exercise the maximal HR is lower in *Clcn2*$^{-/-}$ mice than in *Clcn2*$^{+/+}$ and *Clcn2*$^{+/-}$ mice in all three tests, suggesting that activation of ClC-2 channels in the heart may contribute to the chronotropic response of the mouse to exercise stress. It is possible that activation of ClC-2 channels by β-stimulation induced PKA phosphorylation [35,51,52] may contribute to the regulation of HR during exercise. It has been known that several consensus PKA phosphorylation sites are well conserved in the ClC-2 sequences from different species [35].

Significance

For the first time our results provide strong evidence for the molecular and functional expression of ClC-2 encoded endogenous Cl,ir channels in the SAN cells. The significance of $I_{Cl,ir}$ in the heart may become more prominent under stressed or pathological conditions. Our results may also shed new light on understanding mechanisms for arrhythmias such as sinus node dysfunction or sick sinus syndrome [44]. Cardiac ClC-2 channels may thus represent new therapeutic targets for arrhythmias, congestive heart failure, and ischemic heart diseases.

Acknowledgments

This work was supported by NIH Grant HL63914 (to D.D.), National Center for Research Resources P-20 RR-15581 (to D.D., W.J.H., and F.C.B.), and American Heart Association Western States Affiliate Predoctoral Fellowship (to Z.M.H.) and American Heart Association Western States Affiliate Medical Student Research Award (to C.P.). We are grateful to Dr. Honglin Tian and Lisa Miller for technical assistance. We thank Dr. James Melvin at University of Rochester for providing the *Clcn2*$^{+/-}$ breeders.

References

1. Carmeliet EE. Chloride ions and the membrane potential of Purkinje fibres. J Physiol 1961;156:375–88. [PubMed: 13690854]
2. Hutter O, Noble D. Anion conductance of cardiac muscle. J Physiol 1961;157:335–50. [PubMed: 13717087]
3. Noma A, Irisawa H. Membrane currents in the rabbit sinoatrial node cell as studied by the double microelectrode method. Pflugers Arch 1976;364(1):45–52. [PubMed: 986617]
4. Seyama I. Characteristics of the anion channel in the sino-atrial node cell of the rabbit. J Physiol 1979;294:447–60. [PubMed: 512952]
5. De Mello WC. Role of chloride ions in cardiac action and pacemaker potentials. Am J Physiol 1963;205:567–75. [PubMed: 14065910]
6. Duan D, Liu LL, Bozeat N, Huang ZM, Xiang SY, Wang GL, et al. Functional role of anion channels in cardiac diseases. Acta Pharmacol Sin 2005;26:265–78. [PubMed: 15715921]
7. Hume JR, Duan D, Collier ML, Yamazaki J, Horowitz B. Anion transport in heart. Physiol Rev 2000;80:31–81. [PubMed: 10617765]
8. Britton FC, Wang GL, Huang ZM, Ye L, Horowitz B, Hume JR, et al. Functional characterization of novel alternatively spliced ClC-2 chloride channel variants in the heart. J Biol Chem 2005;280:25871–80. [PubMed: 15883157]
9. Duan D, Ye L, Britton F, Horowitz B, Hume JR. A novel anionic inward rectifier in native cardiac myocytes. Circ Res 2000;86:E63–E71. [PubMed: 10700456]
10. Komukai K, Brette F, Orchard CH. Electrophysiological response of rat atrial myocytes to acidosis. Am J Physiol Heart Circ Physiol 2002;283:H715–H724. [PubMed: 12124220]
11. Komukai K, Brette F, Pascarel C, Orchard CH. Electrophysiological response of rat ventricular myocytes to acidosis. Am J Physiol Heart Circ Physiol 2002;283:H412–H422. [PubMed: 12063316]
12. Thiemann A, Grunder S, Pusch M, Jentsch TJ. A chloride channel widely expressed in epithelial and non-epithelial cells. Nature 1992;356:57–60. [PubMed: 1311421]

13. Furukawa T, Ogura T, Katayama Y, Hiraoka M. Characteristics of rabbit ClC-2 current expressed in Xenopus oocytes and its contribution to volume regulation. Am J Physiol 1998;274:C500–C512. [PubMed: 9486141]
14. Britton FC, Hatton WJ, Rossow CF, Duan D, Hume JR, Horowitz B. Molecular distribution of volume-regulated chloride channels (ClC-2 and ClC-3) in cardiac tissues. Am J Physiol Heart Circ Physiol 2000;279:H2225–H2233. [PubMed: 11045957]
15. Mangoni ME, Nargeot J. Properties of the hyperpolarization-activated current (I_f) in isolated mouse sino-atrial cells. Cardiovas Res 2001;52:51–64.
16. Denyer JC, Brown HF. Rabbit sino-atrial node cells: isolation and electrophysiological properties. J Physiol 1990;428:405–24. [PubMed: 2231420]
17. Kumar R, Wilders R, Joyner RW, Jongsma HJ, Verheijck EE, Golod DA, et al. Experimental model for an ectopic focus coupled to ventricular cells. Circulation 1996;94:833–41. [PubMed: 8772708]
18. Verheijck EE, Wilders R, Joyner RW, Golod DA, Kumar R, Jongsma HJ, et al. Pacemaker synchronization of electrically coupled rabbit sinoatrial node cells. J Gen Physiol 1998;111:95–112. [PubMed: 9417138]
19. Pena-Munzenmayer G, Catalan M, Cornejo I, Figueroa CD, Melvin JE, Niemeyer MI, et al. Basolateral localization of native ClC-2 chloride channels in absorptive intestinal epithelial cells and basolateral sorting encoded by a CBS-2 domain di-leucine motif. J Cell Sci 2005;118:4243–52. [PubMed: 16155254]
20. Coppen SR, Kodama I, Boyett MR, Dobrzynski H, Takagishi Y, Honjo H, et al. Connexin45, a major connexin of the rabbit sinoatrial node, Is co-expressed with connexin43 in a restricted zone at the nodal–crista terminalis border. J Histochem Cytochem 1999;47:907–18. [PubMed: 10375379]
21. Boyett MR, Inada S, Yoo S, Li J, Liu J, Tellez J, et al. Connexins in the sinoatrial and atrioventricular nodes. Adv Cardiol 2006;42:175–97. [PubMed: 16646591]
22. Nehrke K, Arreola J, Nguyen HV, Pilato J, Richardson L, Okunade G, et al. Loss of hyperpolarization-activated Cl^- current in salivary acinar cells from Clcn2 knockout mice. J Biol Chem 2002;277:23604–11. [PubMed: 11976342]
23. Mitchell GF, Jeron A, Koren G. Measurement of heart rate and Q-T interval in the conscious mouse. Am J Physiol 1998;274:H747–H751. [PubMed: 9530184]
24. Duan D, Fermini B, Nattel S. Alpha-adrenergic control of volume-regulated Cl^- currents in rabbit atrial myocytes. Characterization of a novel ionic regulatory mechanism. Circ Res 1995;77:379–93. [PubMed: 7542183]
25. Duan D, Winter C, Cowley S, Hume JR, Horowitz B. Molecular identification of a volume-regulated chloride channel. Nature 1997;390:417–21. [PubMed: 9389484]
26. DiFrancesco D. Funny channels in the control of cardiac rhythm and mode of action of selective blockers. Pharmacol Res 2006;53:399–406. [PubMed: 16638640]
27. Shen JB, Jiang B, Pappano AJ. Comparison of L-type calcium channel blockade by nifedipine and/or cadmium in guinea pig ventricular myocytes. J Pharmacol Exp Ther 2000;294:562–70. [PubMed: 10900233]
28. Vaughan-Jones RD. Chloride activity and its control in skeletal and cardiac muscle. Philos Trans R Soc Lond B Biol Sci 1982;299:537–48. [PubMed: 6130545]
29. Maier SKG, Westenbroek RE, Yamanushi TT, Dobrzynski H, Boyett MR, Catterall WA, et al. An unexpected requirement for brain-type sodium channels for control of heart rate in the mouse sinoatrial node. PNAS 2003;100:3507–12. [PubMed: 12631690]
30. Duan D, Zhong J, Hermoso M, Satterwhite CM, Rossow CF, Hatton WJ, et al. Functional inhibition of native volume-sensitive outwardly rectifying anion channels in muscle cells and Xenopus oocytes by anti-ClC-3 antibody. J Physiol 2001;531:437–44. [PubMed: 11230516]
31. Jarnot MD, Corbett AM. High titer antibody to mammalian neuronal sodium channels produces sustained channel block. Brain Res 1995;674:159–62. [PubMed: 7773687]
32. Duan D, Cowley S, Horowitz B, Hume JR. A serine residue in ClC-3 links phosphorylation-dephosphorylation to chloride channel regulation by cell volume. J Gen Physiol 1999;113:57–70. [PubMed: 9874688]

33. Rees SA, Vandenberg JI, Wright AR, Yoshida A, Powell T. Cell swelling has differential effects on the rapid and slow components of delayed rectifier potassium current in guinea pig cardiac myocytes. J Gen Physiol 1995;106:1151–70. [PubMed: 8786354]
34. Cuppoletti J, Tewari KP, Sherry AM, Kupert EY, Malinowska DH. ClC-2 Cl− channels in human lung epithelia: activation by arachidonic acid, amidation, and acid-activated omeprazole. Am J Physiol Cell Physiol 2001;281:C46–C54. [PubMed: 11401826]
35. Cuppoletti J, Tewari KP, Sherry AM, Ferrante CJ, Malinowska DH. Sites of protein kinase A activation of the human ClC-2 Cl(−) channel. J Biol Chem 2004;279:21849–56. [PubMed: 15010473]
36. Fewell JG, Osinska H, Klevitsky R, Ng W, Sfyris G, Bahrehmand F, et al. A treadmill exercise regimen for identifying cardiovascular phenotypes in transgenic mice. American Journal of Physiology-Heart and Circulatory Physiology 1997;42:H1595–H1605.
37. Desai KH, Sato R, Schauble E, Barsh GS, Kobilka BK, Bernstein D. Cardiovascular indexes in the mouse at rest and with exercise: new tools to study models of cardiac disease. Am J Physiol 1997;272:H1053–H1061. [PubMed: 9124413]
38. Seyama I. The effect of Na, K and Cl ions on the resting membrane potential of sino-atrial node cell of the rabbit. Jpn J Physiol 1977;27:577–88. [PubMed: 604587]
39. Brown HF, Giles W, Noble SJ. Membrane currents underlying activity in frog sinus venosus. J Physiol 1977;271:783–816. [PubMed: 303699]
40. Frace AM, Maruoka F, Noma A. Control of the hyperpolarization-activated cation current by external anions in rabbit sino-atrial node cells. J Physiol 1992;453:307–18. [PubMed: 1281504]
41. Baumgarten CM, Fozzard HA. Intracellular chloride activity in mammalian ventricular muscle. Am J Physiol 1981;241:C121–C129. [PubMed: 6974504]
42. Zhang Z, Xu Y, Song H, Rodriguez J, Tuteja D, Namkung Y, et al. Functional Roles of Cav1.3 (α1D) calcium channel in sinoatrial nodes: insight gained using gene-targeted null mutant mice. Circ Res 2002;90:981–7. [PubMed: 12016264]
43. Bers DM. The beat goes on: diastolic noise that just won't quit. Circ Res 2006;99:921–3. [PubMed: 17068299]
44. Dobrzynski H, Boyett MR, Anderson RH. New insights into pacemaker activity: promoting understanding of sick sinus syndrome. Circulation 2007;115:1921–32. [PubMed: 17420362]
45. Liu J, Noble PJ, Xiao G, Abdelrahman M, Dobrzynski H, Boyett MR, et al. Role of pacemaking current in cardiac nodes: Insights from a comparative study of sinoatrial node and atrioventricular node. Prog Biophys Mol Biol 2007;96:294–304. [PubMed: 17905415]
46. Verkerk AO, Wilders R, Zegers JG, van Borren MM, Ravesloot JH, Verheijck EE. Ca(2+)-activated Cl(−) current in rabbit sinoatrial node cells. J Physiol 2002;540:105–17. [PubMed: 11927673]
47. Hagiwara N, Masuda H, Shoda M, Irisawa H. Stretch-activated anion currents of rabbit cardiac myocytes. J Physiol 1992;456:285–302. [PubMed: 1284078]
48. Staley K, Smith R, Schaack J, Wilcox C, Jentsch TJ. Alteration of GABAA receptor function following gene transfer of the CLC-2 chloride channel. Neuron 1996;17:543–51. [PubMed: 8816717]
49. Ohba M. Effects of tonicity on the pacemaker activity of guinea-pig sino-atrial node. Jpn J Physiol 1986;36:1027–38. [PubMed: 2435940]
50. Carmeliet E. Cardiac ionic currents and acute ischemia: from channels to arrhythmias. Physiol Rev 1999;79:917–1017. [PubMed: 10390520]
51. Fritsch J, Edelman A. Modulation of the hyperpolarization-activated Cl^- current in human intestinal T84 epithelial cells by phosphorylation. J Physiol 1996;490:115–28. [PubMed: 8745282]
52. Sherry AM, Stroffekova K, Knapp LM, Kupert EY, Cuppoletti J, Malinowska DH. Characterization of the human pH- and PKA-activated ClC-2G (2 α) Cl^- channel. Am J Physiol 1997;273:C384–C393. [PubMed: 9277336]

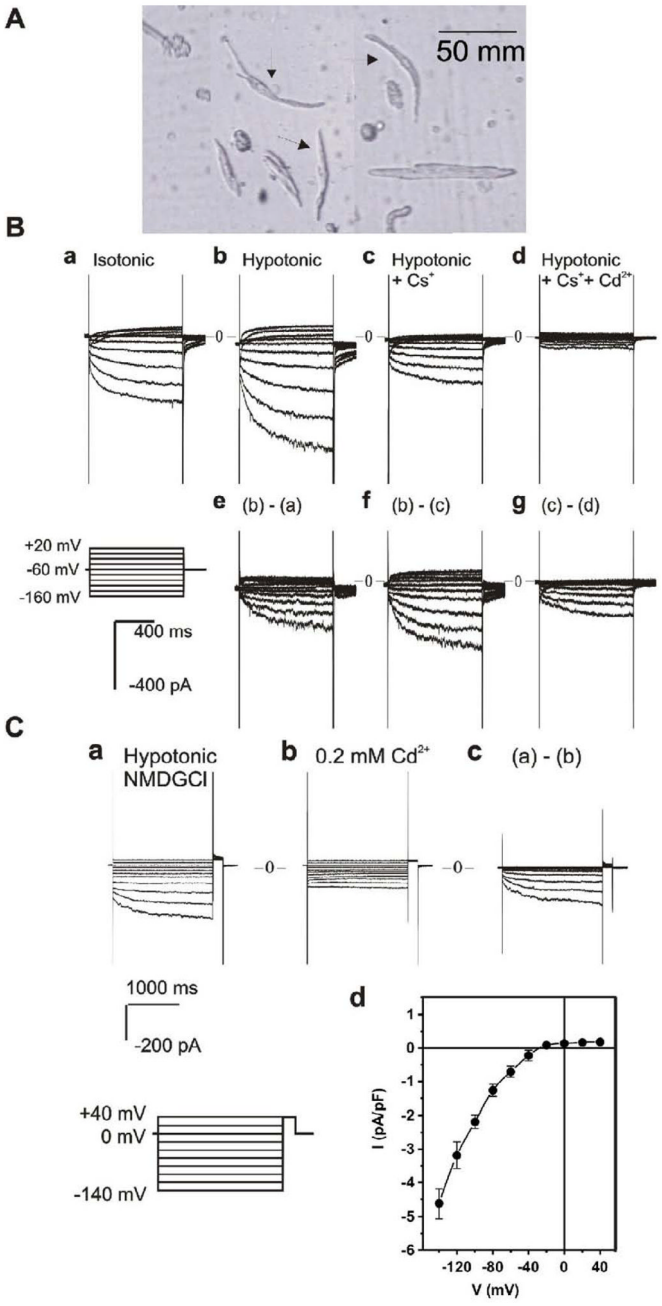

Figure 1. Whole-cell currents recorded from SAN cells of guinea-pig heart

A. Single SAN cells isolated from the SAN region of guinea-pig heart by enzymatic dispersion. Note the morphology used to identify the SA nodal cells (spindle-shaped, 4–10 μm wide and 50–100 μm long, and with a smooth surface) as indicated by the arrows. The atrial cells seen adjacent to the SAN cells are well-striated and bigger in size. **B.** Typical whole-cell currents recorded from SAN cells in 5 experiments. When Na^+ and K^+ were included in the extracellular solutions, inward currents were slowly activated upon hyperpolarization under isotonic (**a**) conditions. Exposure of the same cell to hypotonic extracellular solution caused cell swelling and an increase in the inward current amplitude (**b**). The difference current caused by hypotonic cell swelling is shown in panel **e**. Subsequent replacement of 20 mM of NaCl with CsCl caused

a significant inhibition of the inward current (**c**). The Cs^+-sensitive current is shown in panel **f**. Subsequent addition of 0.2 mM of Cd^{2+} to the hypotonic solution caused an inhibition of the inward current (**d**). The Cd^{2+}-sensitive currents are shown in panel **g**. Voltage protocol is shown in the insert. **C.** Whole cell currents recorded from SAN cells when all cations in both extracellular and intracellular solutions were replaced by impermeable NMDG. Under hypotonic conditions, hyperpolarization activated a time-dependent inward current (**a**), which was sensitive to inhibition by 0.2 mM of Cd^{2+} (**b**). Panel **c** shows the difference current (a–b) inhibited by Cd^{2+}. The voltage protocol for the current recordings is shown in the insert. The mean *I–V* relation of the Cd^{2+} sensitive currents recorded from 5 different cells under the same conditions is shown in panel **d**.

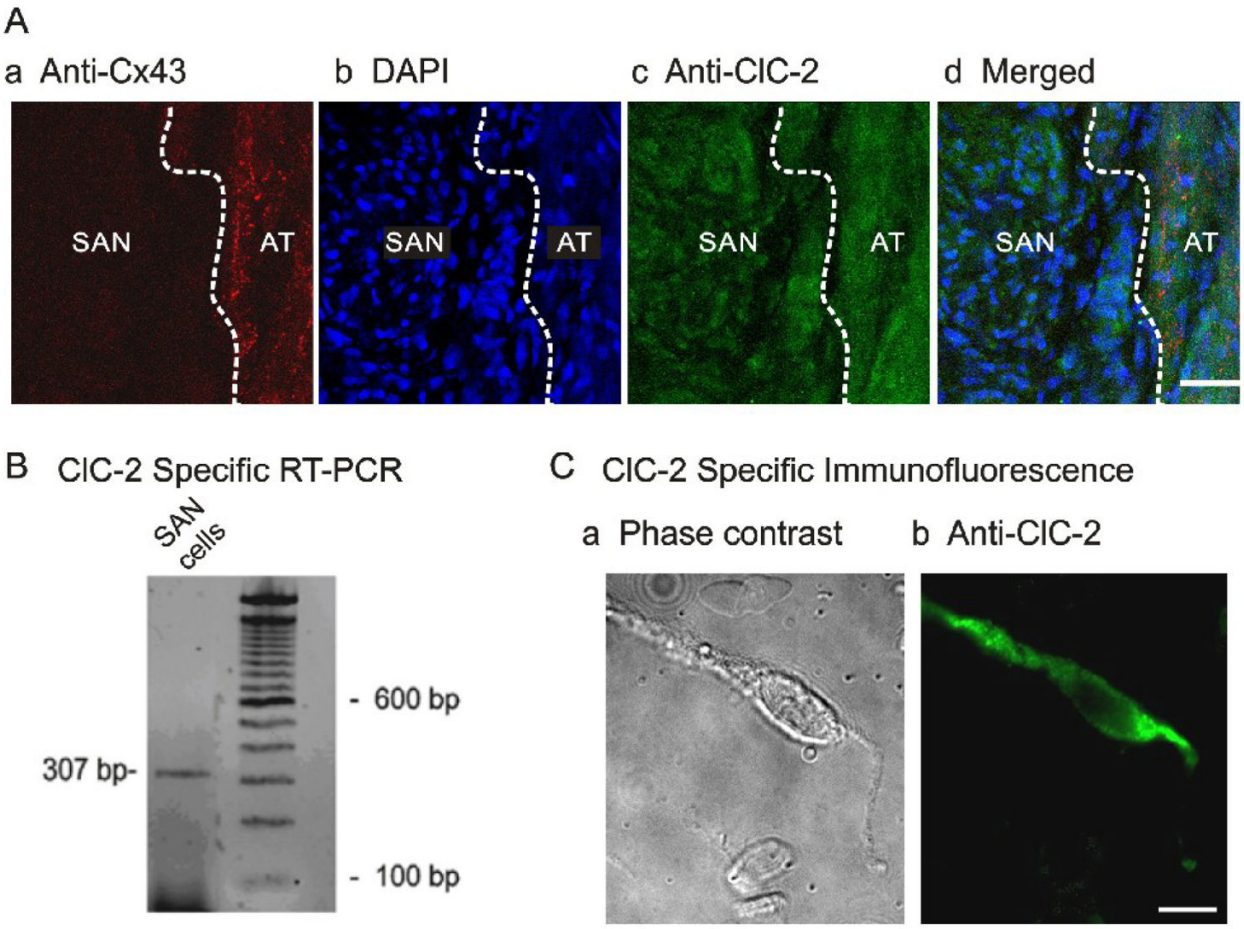

Figure 2. Molecular expression of *ClC-2* in SAN cells. A

Localization of *ClC-2* chloride channels in guinea-pig SAN tissue. **a**) Section labeled with anti-Connexin 43 (red) to illustrate the adjacent atrial (AT) septum was positively labelled while the SAN was negative (dark region), which clearly delineates the SAN region from the AT septum (dashed white line). **b)** Section stained with DAPI (blue) to compare nuclei density in the SAN region and in AT. The SAN region had a higher DAPI staining density (higher nuclei density) than the adjacent AT. **c**) Section stained with anti-*ClC-2* (green). ClC-2 immunoreactivity is evident in both SAN and AT regions. **d**) Merged images of **a**, **b**, and **c** illustrate that *ClC-2* is expressed in the densely nucleated and Cx43 negative SAN region. **B.** Agarose gel depicting RT-PCR product of *ClC-2* amplified from mRNA prepared from enzymatically dispersed guinea-pig SA nodal cells. **C.** Images of ClC-2-like immunofluorescence in a representative SAN cell visualized using fluorescent microscopy. Phase contrast (**a**) and fluorescent micrographs (**b**) of a single SAN cell.

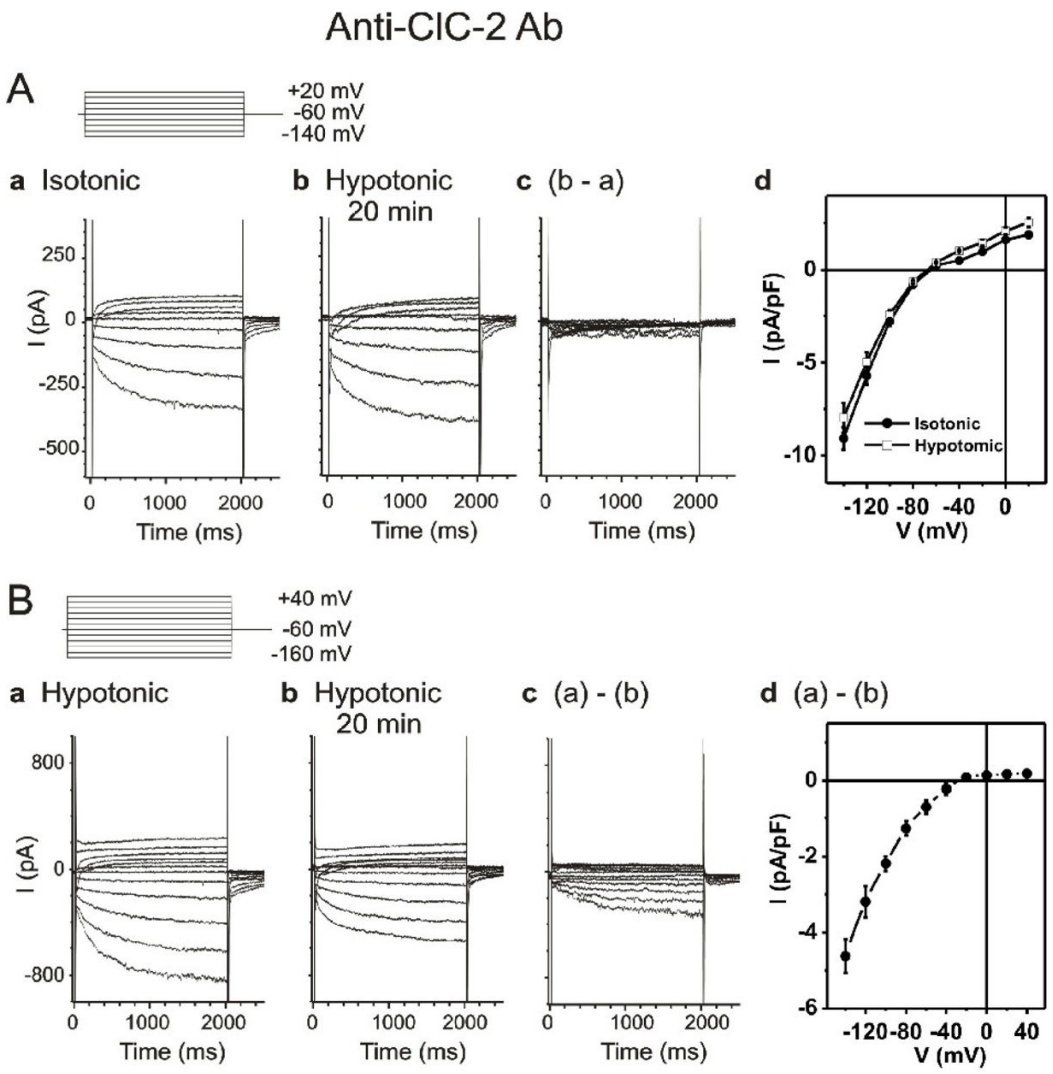

Figure 3. Effects of Anti-*ClC-2* Ab on $I_{Cl,ir}$ in SAN cells

A. Representative whole-cell currents recorded from SAN cells under isotonic (panel **a**) and hypotonic (panel **b**) conditions in the presence of anti-ClC-2 Ab in the pipette solutions. SAN cells were exposed to isotonic solution for at least 10 min before whole-cell recordings. Currents shown in panel **a** were recorded right after successful whole-cell configuration under isotonic conditions. Currents shown in panel **b** were recorded after exposure to hypotonic solution for 20 min. Pipette and bath solutions were identical to those described in Figure 1B except the pipette solution contained 3 μg/ml anti-ClC-2 Ab. **d.** Mean *I–V* from 5 SAN cells under the same conditions. **B.** SAN cells were exposed to hypotonic solution for 20 min to fully activate $I_{Cl,ir}$ before whole-cell recordings. Bath and pipette solutions were the same as in panel A. Representative current traces recorded by voltage-clamp (protocol is shown in insert) from the SAN cell immediately after membrane rupture (**a**) and after 20 min of anti-ClC-2 Ab dialysis (**b**). The anti-ClC-2 Ab-sensitive current (**a**)–(**b**) is shown in **(c)** (current traces) and **(d)** (mean *I–V*, n=5**)**. Notice the anti-ClC-2 Ab-sensitive current (**c**) was similar to $I_{Cl,ir}$ shown in Figure 1 and the typical I_{Ca} and I_f(**b**) were not affected by anti-ClC-2 Ab.

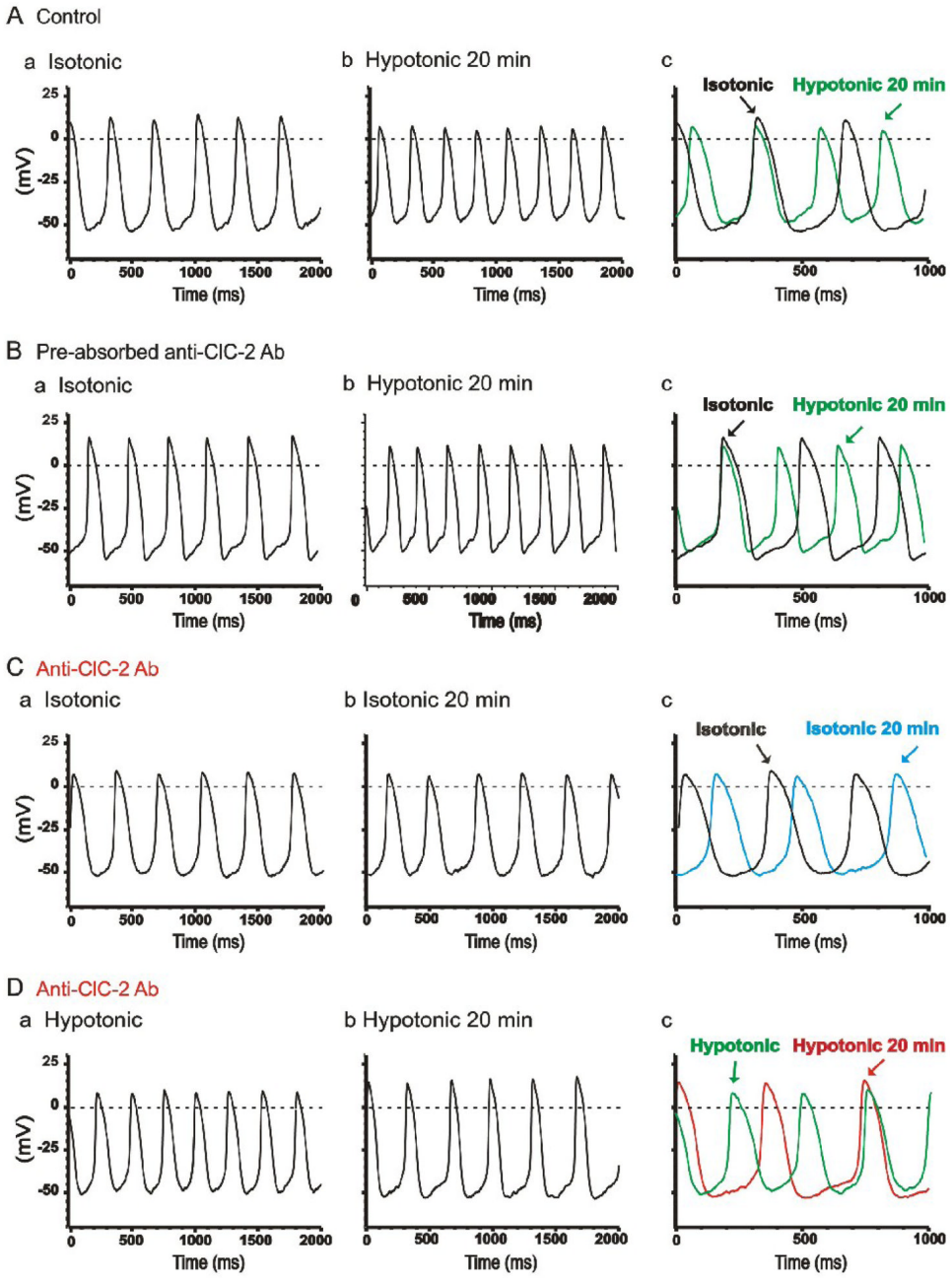

Figure 4. Effects of Anti-*ClC-2* Ab on pacemaker action potential in SAN cells

A. Representative spontaneous action potentials recorded from an SAN cell by current-clamp (no current injection) with pipette solution containing no anti-*ClC-2* Ab under isotonic (**a**) and hypotonic (**b**) conditions. SAN cells were exposed to isotonic solution for at least 10 min before action potential recordings. Action potentials shown in panel **a** were recorded right after successful whole-cell configuration under isotonic conditions. Action potentials shown in panel **b** were recorded after exposure to hypotonic solution for 20 min. For comparison, the action potentials recorded under these conditions were superimposed with an expanded time scale in panel **c**. The dotted lines indicate zero voltage. **B.** Spontaneous action potentials recorded from a SAN cell by current-clamp using a pipette solution containing pre-absorbed

anti-*ClC-2* Ab (control) and cell was exposed to isotonic solutions for 10 min (**a**) and hypotonic solutions for 20 min (**b**). For comparison, the action potentials recorded under these conditions were superimposed with an expanded time scale in panel **c. C**. SAN cells were perfused with isotonic solutions for 20 min before whole-cell recordings. Action potentials were recorded immediately after membrane rupture (**a**) and after dialysis of anti-*ClC-2* Ab for 20 min (**b**) under the same isotonic conditions. Panel **c** shows the expanded and superimposed action potentials as shown in panel **a** and panel **b**. Note that after 20 min dialysis of anti-*ClC-2* Ab in to the cell the spontaneous action potential rate was not significantly altered. **D**. SAN cells were exposed to hypotonic solution for 20 min to fully activate $I_{Cl,ir}$ before whole-cell recordings. Action potentials were recorded immediately after membrane rupture (**a**) and after dialysis of anti-*ClC-2* Ab for 20 min (**b**). Panel **c** shows the expanded and superimposed action potentials as shown in panel **a** and panel **b**. Note that the spontaneous action potential rate significantly decreased after 20 min dialysis of anti-*ClC-2* Ab in to the cell, which corresponds with the decrease in inward current as shown in Figure 3**B,b**.

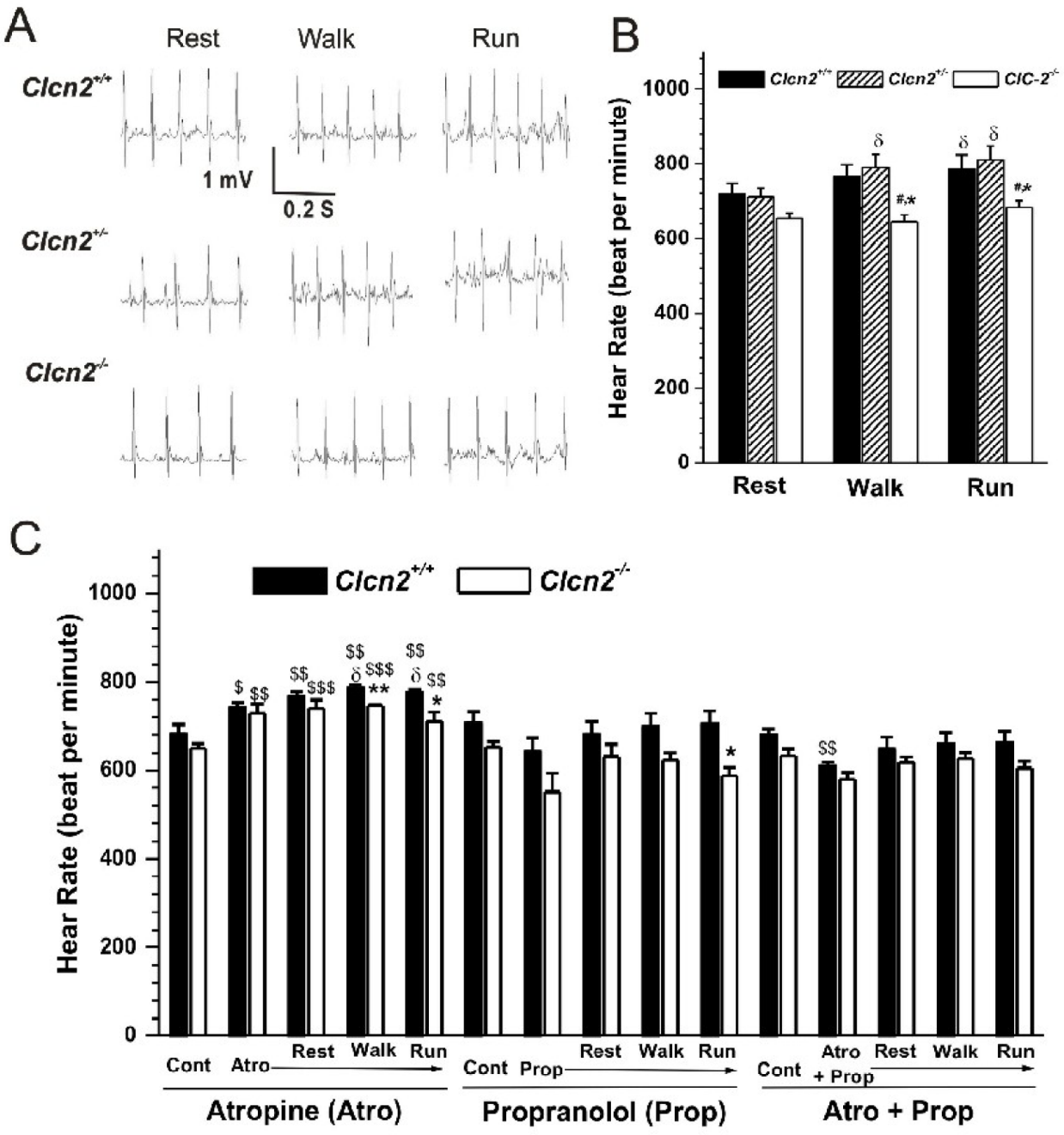

Figure 5. Telemetry ECG recordings in *Clcn2*$^{-/-}$ mice and their *Clcn2*$^{+/+}$ and *Clcn2*$^{+/-}$ littermates during treadmill exercises

A. Representative ECG (Lead II) recordings in *Clcn2*$^{+/+}$, *Clcn2*$^{+/-}$, and *Clcn2*$^{-/-}$ mice while they were subjected to treadmill exercise at a) Rest period: acclimation at 0 m/min, incline 0 ° for 5 min; b) Walk period: walking at 5m/min, incline 0 ° for 5 min; c) Run period: running at 15 m/min, uphill incline 8 ° for 5 min. **B**. Mean heart rate during the last minute of each treadmill exercise segment for the *Clcn2*$^{+/+}$ (n=6), *Clcn2*$^{+/-}$ (n=5), and *Clcn2*$^{-/-}$ (n=7) mice. **C**. Mean heart rate of the *Clcn2*$^{+/+}$ (n=5) and *Clcn2*$^{-/-}$ (n=4) mice before (Control, Cont) and after the intraperitoneal injection of atropine (Atro), propranolol (Prop), or atropine plus propranolol (Atro + Prop) during the last minute of each treadmill exercise segment (Rest,

Walk, and Run). * $P < 0.05$, ** $P < 0.01$, *** $P < 0.001$ vs *Clcn2*$^{+/+}$, $^{\#}P < 0.05$, $^{\#\#}P < 0.01$, $^{\#\#\#}P < 0.001$ vs *Clcn2*$^{+/-}$; $^{\$}P < 0.05$, $^{\$\$}P < 0.01$, $^{\$\$\$}P < 0.001$ vs control (Cont); $^{\delta}P < 0.05$ vs Rest.

Table 1

Action potential characteristics of SAN cells with and without inhibition of ClC-2 by anti-*ClC-2* antibody (Ab) under isotonic or hypotonic conditions.

	Control (n = 4)			**Pre-absorbed anti-*ClC-2* Ab (n = 4)**			**Anti-*ClC-2* Ab (n = 4)**			**Anti-*ClC-2* Ab (n = 7)**		
	Isotonic	**Hypotonic 20 min**	***P***	**Isotonic**	**Hypotonic 20 min**	***P***	**Isotonic**	**Isotonic 20 min**	***P***	**Hypotonic**	**Hypotonic 20 min**	***P***
CL (ms)	336.6±19.2	269.0±3.4	*	319.1±6.5	277.1±7.2	**	314.1±4.9	327.1±4.6	NS	255.7±6.5	308.2±8.6	***, ##, §
MDP (mV)	−57.4±1.2	−49.1±1.6	**	−58.4±2.0	−52.1±1.5	*	−58.4±1.7	−58.2±1.4	NS	−54.5±1.1	−60.4±1.1	**, ###, §§
APA (mV)	69.9±3.2	59.5±2.4	*	74.9±2.1	68.8±1.3	*	69.9±1.3	70.5±1.1	NS	65.4±2.0	73.5±1.2	**, ###, §
APD50 (ms)	89.9±3.9	63.8±2.0	***	86.8±1.6	71.8±3.1	**	86.8±1.6	88.1±2.8	NS	70.1±1.7	87.4±2.4	***, ###, §§
APD90 (ms)	121.9±4.4	95.5±3.4	**	114.6±2.9	93.3±2.8	**	114.6±2.8	121.0±5.2	NS	101.0±1.9	127.9±3.2	***, ###, §§
DDs (mV/s)	44.6±2.8	64.6±3.9	**	47.0±2.9	62.2±2.4	**	47.0±2.9	45.6±1.8	NS	62.3±2.8	47.6±1.9	***, ###, §§

CL (ms): cycle length; MDP (mV): maximum diastolic potential; APA: action potential amplitude; APD_{50} (ms) and APD_{90} (ms): action potential at 50 and 90% repolarization, respectively; DDs (mV/s): diastolic depolarization slope.

$^{*}P<0.05$,

$^{**}P<0.01$,

$^{***}P<0.001$ hypotonic 20 min vs isotonic (control and pre-absorbed anti-*ClC-2* Ab) or hypotonic (anti-*ClC-2* Ab); NS: not significant isotonic 20 min vs isotonic;

$^{\#}P<0.05$,

$^{\#\#}P<0.01$,

$^{\#\#\#}P<0.001$ anti-*ClC-2* Ab/hypotonic 20 min vs Control/hypotonic 20 min;

$^{\S}P<0.05$,

$^{\S\S}P<0.01$,

$^{\S\S\S}P<0.001$ anti-*ClC-2* Ab/hypotonic 20 min vs pre-absorbed anti-*ClC-2* Ab/hypotonic 20 min. No significant differences (ANOVA) were found 1) among Control/hypotonic 20 min, pre-absorbed anti-*ClC-2* Ab/hypotonic 20 min, and anti-*ClC-2* Ab/hypotonic; 2) among Control/isotonic, pre-absorbed anti-*ClC-2* Ab/isotonic and anti-*ClC-2* Ab/isotonic; 3) between pre-absorbed anti-*ClC-2* Ab/hypotonic 20 min and Control/hypotonic 20 min; and 4) between anti-*ClC-2* Ab/hypotonic 20 min and. anti-*ClC-2* Ab/isotonic 20 min.